Fullerene-assisted electron-beam lithography for pattern improvement and loss reduction in InP membrane waveguide devices

DOI:
10.1364/OL.39.001645

Fullerene-assisted electron-beam lithography for pattern improvement and loss reduction in InP membrane waveguide devices

Yuqing Jiao,* Josselin Pello, Alonso Millan Mejia, Longfei Shen, Barry Smalbrugge, Erik Jan Geluk, Meint Smit, and Jos van der Tol

COBRA Research Institute, Eindhoven University of Technology, P.O. Box 513, Eindhoven 5600 MB, The Netherlands
**Corresponding author: y.jiao@tue.nl*

Received January 27, 2014; revised February 16, 2014; accepted February 16, 2014; posted February 18, 2014 (Doc. ID 204076); published March 13, 2014

In this Letter, we present a method to prepare a mixed electron-beam resist composed of a positive resist (ZEP520A) and C_{60} fullerene. The addition of C_{60} to the ZEP resist changes the material properties under electron beam exposure significantly. An improvement in the thermal resistance of the mixed material has been demonstrated by fabricating multimode interference couplers and coupling regions of microring resonators. The fabrication of distributed Bragg reflector structures has shown improvement in terms of pattern definition accuracy with respect to the same structures fabricated with normal ZEP resist. Straight InP membrane waveguides with different lengths have been fabricated using this mixed resist. A decrease of the propagation loss from 6.6 to 3.3 dB/cm has been demonstrated.

OCIS codes: (110.4235) Nanolithography; (130.3120) Integrated optics devices; (230.7370) Waveguides.
http://dx.doi.org/10.1364/OL.39.001645

The ever-growing demand for high-speed chip-scale data transport in computers has inspired the development of on-chip optical interconnects [1]. The InP membrane on Si (IMOS) technology [2] is a novel concept for realizing such a photonic interconnect layer on top of a conventional complementary metal oxide semiconductor (CMOS) circuit. Compared to other concepts such as III-V bonded on silicon-on-insulator [3] or Si/Ge [4], the major advantage of the IMOS technology is the potential to realize monolithic III-V active–passive integration with both compact passive photonic devices and high-performance active devices.

The IMOS passive waveguides and devices can be fabricated using electron-beam lithography (EBL) with ZEP520A resist. During the characterization of previously fabricated devices we have observed a relatively high propagation loss of the InP membrane waveguides. The average propagation loss is around 10–15 dB/cm with a best result of 6.6 dB/cm. This loss is suspected to be mostly caused by the sidewall roughness on the ZEP resist pattern after exposure and development. Furthermore the erosion on the resist pattern when using it as a plasma etching mask increases the roughness. Such high propagation loss will significantly limit the performance of both active and passive InP membrane devices. Therefore it is crucial to develop an improved electron-beam resist with reduced roughness.

One of the practical approaches to loss reduction is to use the so-called fullerene-assisted resist system [5]. The incorporation of fullerene in a resist system can improve the material strength during plasma etching [e.g., reactive ion etching (RIE)] as well as wet chemical etching (e.g., developer solution) [5]. As a result, a reduced sidewall roughness of the resist pattern can be obtained. A reduction of the waveguide propagation loss has been experimentally demonstrated for Si wire waveguides (4.5 dB/cm [6]) and InGaAsP wire waveguides (4 dB/cm [7]), by incorporating C_{60} (one of the fullerene types) into the ZEP resist.

In this Letter, we present a method to prepare such C_{60}-assisted ZEP resist and use it in an EBL process for realizing InP membrane devices. We show the change of the resist properties due to the presence of the C_{60} material as well as the improved pattern definition due to the changed properties. Finally we demonstrate the reduction of the waveguide propagation loss (3.3 dB/cm) using this mixed resist. This loss value is, to our knowledge, the lowest value so far obtained for InP membrane waveguides. Moreover, our C_{60}-assisted EBL process does not require extra dose corrections on the waveguide edges [6] or multilayer resists [7].

The preparation procedure of the C_{60}/ZEP mixed resist is similar to what has been described in [5]. However, the preparation method in [5] uses ortho-dichlorobenzene (*o*-DCB) as the solvent for dissolving C_{60}, since *o*-DCB was once the solvent for ZEP520A resist. Nowadays *o*-DCB is not preferred in many cleanrooms because of its high toxicity. In our case, the C_{60} powder is first dissolved in anisole (solubility is about 5.6 g per liter [8]), which has a relatively low toxicity, and then mixed with ZEP520A resist solution (with anisole as the solvent) by magnetic stirring and ultrasonic bath. The mass ratio between C_{60} and ZEP material is 1:9. The final mixed solution will appear black due to the presence of C_{60} instead of transparent as for normal ZEP resist.

Since an additional amount of anisole is added as solvent into the mixed resist solution, the concentration of the ZEP material will decrease. As a result the thickness of the mixed resist after spin coating will be less than that of the normal ZEP resist. For instance, the thickness of the mixed resist at a spin speed of 2000 rpm is about 100 nm, while the thickness of the normal ZEP resist at 5000 rpm is 300 nm.

The fabrication of IMOS waveguide devices starts by depositing a 1850 nm thick SiO_2 layer on top of a Si wafer and a 50 nm SiO_2 layer on top of an InP wafer by using plasma-enhanced chemical vapor deposition (PECVD).

The InP wafer contains a 250 nm thick InP membrane layer as the future waveguiding layer and a 300 nm thick InGaAs sacrificial layer between the membrane layer and the substrate. The Si wafer and the InP wafer are adhesively bonded using a 50 nm thick divinylsiloxane-bisbenzocyclobutene (DVS-BCB) layer [9] [see Fig. 1(a)]. After wet-chemically removing the InP substrate and the InGaAs sacrificial layer, the 250 nm thick InP membrane is tightly bonded on top of the SiO_2/Si carrier wafer [see Fig. 1(b)]. The fabrication requires two steps of EBL. Both steps utilize a 50 nm thick PECVD-deposited SiN_x layer on top of the InP membrane as the hard mask for the subsequent etching step. The 100 nm thick mixed resist material is spin coated on top of this SiN_x layer, and the designed patterns are written on the resist layer using a Raith 150-two EBL system with 20 kV voltage and 10 μm aperture settings. The mixed resist contains only a single layer of resist material and does not require any proximity effect corrections during EBL. After development, the patterns on the resist layer are transferred to the SiN_x layer by means of CHF_3 RIE. Finally the patterns are transferred from the SiN_x layer into the InP membrane using CH_4/H_2 InP RIE. The first EBL step [see Fig. 1(c)] prints all the waveguide designs as well as the local markers for alignment of the next EBL step. The final InP waveguides have a width of 400 nm and an etch depth of 220 nm [see Fig. 1(d)]. The second EBL step [see Fig. 1(e)] prints the grating couplers [10] for coupling light between optical fibers and the waveguides. The gratings have a period of 680 nm with 50% filling factor and an etch depth of 100 nm [see Fig. 1(f)]. The gratings have a width of 10 μm and are connected to the waveguides through adiabatic tapers. The processing procedure is the same as for the standard IMOS passive processing [2,11] except for the change of the resist material from normal ZEP to the mixed resist. It is also worth mentioning that our fabricated waveguides do not have a SiO_2 or SiN_x upper cladding layer, as was used in [6] and [7] to reduce the propagation loss.

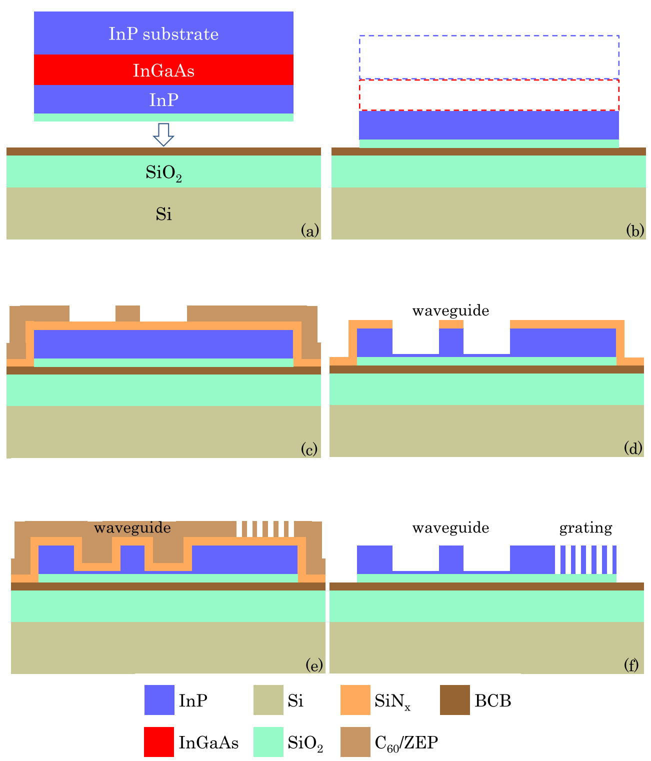

Fig. 1. Process flow for IMOS passive devices. (a) InP wafer bonded to SiO_2/Si carrier wafer. (b) Removal of InP substrate and InGaAs sacrificial layer. (c) First EBL for waveguides. (d) Waveguide etching. (e) Second EBL for gratings. (f) Final IMOS wafer after grating etching.

The addition of C_{60} material in the ZEP resist changes significantly the properties of the resist system regarding the clearing dose during EBL and the thermal behavior. It is found that in the Raith 150-two EBL system with 20 kV voltage and 10 μm aperture settings, the clearing dose of the mixed resist has increased to 48 $\mu C/cm^2$, whereas the normal ZEP resist has a clearing dose of 38 $\mu C/cm^2$. A postexposure bake is crucial for obtaining a smooth resist sidewall. The bake temperature is chosen close to the reflow temperature of the resist so that the roughness on the sidewalls can be smoothened during controlled reflow. After being mixed with C_{60}, the reflow temperature of the mixed resist has increased from 154°C for normal ZEP to 170°C. This is due to the increased thermal strength provided by the C_{60} material. Furthermore, the mixed resist also shows much less deformation after 170°C baking compared to the normal ZEP resist after 154°C baking.

The processing parameters (e.g., clearance dose and baking temperature) for normal ZEP and mixed resist are optimized separately from a series of tests with a scan of processing parameters. The superior results that the mixed resist has achieved could not be reproduced by the normal ZEP resist. The reason is that for the normal ZEP, due to the low thermal resistance, the fine pattern definition (requires reduced baking temperature) and the low propagation loss (requires increased baking temperature) cannot be satisfied at the same time. On the other hand, the mixed resist can have a much better achievement on both pattern definition and loss reduction thanks to its enhanced thermal resistance.

As can be seen from the scanning electron microscope (SEM) picture shown in Fig. 2(a), the corners of a multimode interference (MMI) coupler structure are all rounded due to the reflow of the normal ZEP resist at 154°C. This rounding can reduce the performance of the devices. On the other hand, after 170°C baking, the mixed resist still shows relatively sharp corner, as designed [see Fig. 2(b)].

The improved thermal resistance of the mixed resist also helps to realize structures with narrow gaps. For instance, the coupling regions of microring resonators (MRRs) are fabricated using both mixed resist and normal ZEP and baked at 170°C and 154°C, respectively. The gap of the coupling region is designed to be 50 nm. It can be clearly seen from Figs. 3(a) and 3(b) that the gap in the coupling region fabricated with normal ZEP resist has already closed due to the deformation of the resist during baking. On the other hand, the gap fabricated with the mixed resist survives after baking, with a gap of 90 nm. Thus it is obvious that IMOS photonic devices can be printed more accurately thanks to the thermal resistance enhancement in the mixed resist.

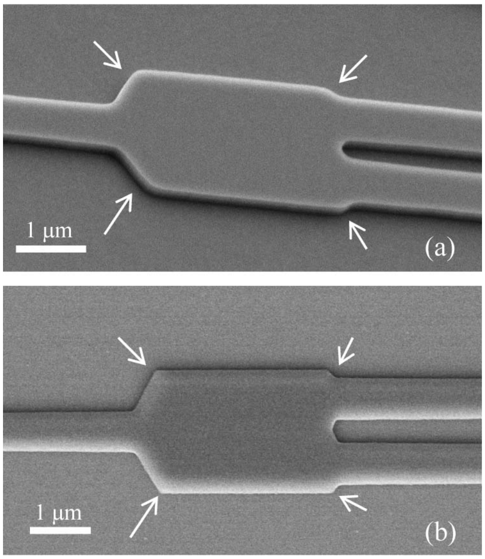

Fig. 2. SEM pictures of the MMI coupler structures fabricated by using (a) normal ZEP resist (b) mixed resist. The corners of the MMIs are highlighted by arrows.

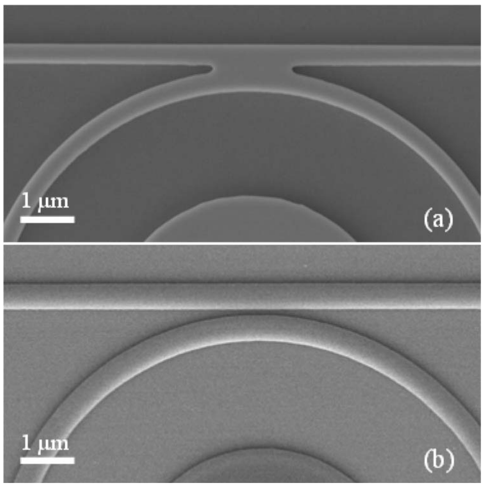

Fig. 3. SEM pictures of the coupling regions of MRRs fabricated by using (a) normal ZEP resist and (b) mixed resist.

The distributed Bragg reflector (DBR) structures used in the IMOS planar concave grating (PCG) demultiplexers [11] have also been fabricated using both pure ZEP and mixed resist. The DBR structure made with the pure ZEP suffers from trench width variation, roughness, and proximity effects during the EBL [see Fig. 4(a)], which results in extra insertion loss [11]. However the DBR structure made with the mixed resist [see Fig. 4(b)] provides excellent pattern definition with a uniform filling factor of the gratings, sharp grating corners, and significant reduction of proximity effects. The reduced thickness of the mixed resist helps to reduce the proximity effects, and the improved thermal resistance helps to preserve the precise patterns after the postexposure bake.

Straight IMOS passive waveguides of different lengths are fabricated using the mixed resist for loss measurement. The fabricated membrane waveguides have two identical sets. Each set contains five different lengths from 140 to 940 μm, with 200 μm increment.

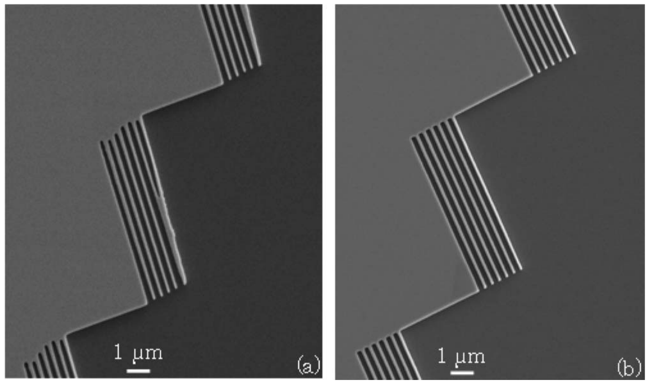

Fig. 4. SEM pictures of the DBR structures in the IMOS PCG devices fabricated by using (a) normal ZEP resist and (b) mixed resist.

The measurement of the waveguide loss is performed using a commercial laser with 1550 nm wavelength and 12 dBm output power in fiber. The laser light is coupled to the input grating coupler by a single-mode fiber with a cleaved facet. The light transmitted to the output grating coupler is collected by another fiber. Both fibers are vertically placed with an angle of 9 deg from the normal direction to the surface of the chip. The output power is measured by a power meter. The measurement result of the insertion loss (including both propagation loss and grating coupling loss) of the 10 waveguides, as a function of the waveguide length, is shown in Fig. 5. The measured data is fitted with a linear function from which a propagation loss of 3.3 dB/cm and a fiber-grating coupling loss of 6.4 dB per grating coupler are extracted. Compared to the propagation loss of more than 10 dB/cm in average, with a best value of 6.6 dB/cm, obtained using the normal ZEP resist, the measured 3.3 dB/cm propagation loss obtained using the mixed resist proves that a significant loss improvement is achieved by the assistance of C_{60} material.

In conclusion, we have developed a method for preparing a mixed resist system with ZEP520A and C_{60} fullerene. The mixed resist shows an increased clearing dose and an enhanced thermal resistance compared to normal ZEP resist. The comparison of IMOS devices fabricated using normal and mixed ZEP resist indicates a significant improvement in the fabrication accuracy with the mixed resist. Loss measurement on the IMOS passive

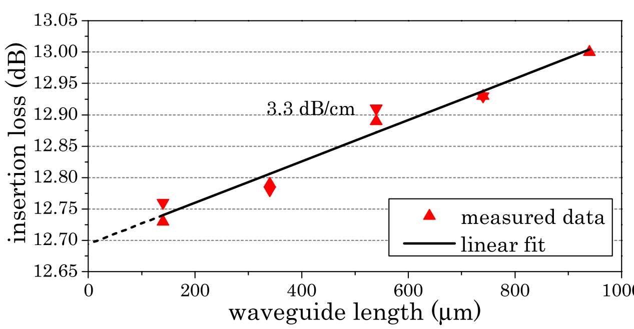

Fig. 5. Measured insertion loss of the IMOS passive waveguides as a function of waveguide length.

waveguides also demonstrates a reduced propagation loss (3.3 dB/cm) with the mixed resist.

The authors acknowledge support from the ERC NOLIMITS project and thank the Nanolab@TU/e for the cleanroom facilities.

References

1. M. Haurylau, G. Chen, H. Chen, J. Zhang, N. A. Nelson, D. H. Albonesi, E. G. Friedman, and P. M. Fauchet, IEEE J. Sel. Top. Quantum Electron. **12**, 1699 (2006).
2. J. van der Tol, R. Zhang, J. Pello, F. Bordas, G. Roelkens, H. Ambrosius, P. Thijs, F. Karouta, and M. Smit, IET Optoelectron. **5**, 218 (2011).
3. D. Liang, G. Roelkens, R. Baets, and J. Bowers, Materials **3**, 1782 (2010).
4. S. Assefa, F. Xia, and Y. A. Vlasov, Nature **464**, 80 (2010).
5. T. Ishii and K. Shigehara, in *Hybrid Nanocomposites for Nanotechnology*, L. Merhari, ed. (Springer, 2009), pp. 387–427.
6. K. Inoue, D. Plumwongrot, N. Nishiyama, S. Sakamoto, H. Enomoto, S. Tamura, T. Maruyama, and S. Arai, Jpn. J. Appl. Phys. **48**, 030208 (2009).
7. J. Lee, Y. Maeda, Y. Atsumi, Y. Takino, N. Nishiyama, and S. Arai, Jpn. J. Appl. Phys. **51**, 042201 (2012).
8. R. S. Ruoff, D. S. Tse, R. Malhotra, and D. C. Lorents, J. Phys. Chem. **97**, 3379 (1993).
9. S. Keyvaninia, M. Muneeb, S. Stankovi, P. J. Van Veldhoven, D. Van Thourhout, and G. Roelkens, Opt. Mater. Express **3**, 35 (2013).
10. D. Taillaert, W. Bogaerts, P. Bienstman, T. F. Krauss, P. van Daele, I. Moerman, S. Verstuyft, K. De Mesel, and R. Baets, IEEE J. Quantum Electron. **38**, 949 (2002).
11. J. Pello, M. Muneeb, S. Keyvaninia, J. J. G. M. van der Tol, G. Roelkens, and M. K. Smit, IEEE Photon. Technol. Lett. **25**, 1969 (2013).